IEEE Access
Multidisciplinary | Rapid Review | Open Access Journal

Received 23 May 2023, accepted 6 June 2023, date of publication 19 June 2023, date of current version 26 June 2023.

Digital Object Identifier 10.1109/ACCESS.2023.3287322

RESEARCH ARTICLE

Research on Fault Location in DC Distribution Network Based on Adaptive Artificial Bee Colony Slime Mould Algorithm

TIAN-XIANG MA[1], XIN DUAN[1], YAN XU[2], RUO-LIN WANG[2], AND XIAO-YU LI[1]

[1]State Grid Hebei Electric Power Research Institute, Shijiazhuang 050021, China
[2]State Key Laboratory of Alternate Electrical Power System with Renewable Energy Sources, North China Electric Power University (Baoding), Baoding 071003, China

Corresponding author: Tian-Xiang Ma (843419784@qq.com)

This work was supported by the Science and Technology Project of State Grid Corporation of China (SGCC) under Grant kj2021-003.

ABSTRACT To address the problems of slow convergence speed, easy to fall into local minima and low convergence accuracy presented by previous algorithms in DC distribution network fault location, this paper adopts the improved artificial bee colony slime mould algorithm (SMA) to improve and solve. On the basis of SMA, an adaptive adjustable feedback factor and an improved crossover operator are introduced to improve the convergence speed; artificial bee colony (ABC) algorithm is introduced to improve the search ability to jump out of local minima, and the artificial bee colony slime mould algorithm (ISMA) is formed. Firstly, based on the six-terminal DC distribution network topology, a mathematical model of bipolar short-circuit fault as well as single-pole grounded short-circuit fault is established based on a fault occurring between G-VSC and W-VSC as an example. Then the principle of the improved ISMA is introduced in detail, and a suitable fitness function is established as the measure of fault location in DC distribution network. Finally, experimental simulations are conducted to obtain fault points from the optimization search and compare them with the actual values to verify the accuracy of the algorithm. In addition, the efficiency and robustness of ISMA are further verified by comparing with other algorithms.

INDEX TERMS Distribution network, fault location, parameter identification, DC distribution system, artificial bee colony slime mould algorithm.

I. INTRODUCTION

Because of their numerous advantages, metaheuristic algorithms (MAs) have become widely used in a variety of fields in recent decades [1]. The stochastic factor prevents the algorithm from falling into local optimal solutions, so MAs require less information than traditional gradient descent algorithms. However, the MA's convergence speed is slower than that of the gradient descent method. The gradient descent method is commonly used to solve linear problems. MAs provide a large, random solution space in the space when solving nonlinear problems, replacing the method of traversing the solution and detecting the optimal solution under limited conditions. Genetic Algorithms (GA), Genetic Programming (GP), and Evolutionary Algorithms(EA) are three popular algorithms. Swarm Intelligence(SI) includes collective or social intelligence, which artificially simulates the collective behavior of biological clusters in nature's decentralized or self-organized systems [2]. Inspiration for this type of algorithm typically comes from groups of organisms in nature that have collective behavior and intelligence to achieve specific goals. SI algorithms are simpler to implement and require fewer operators to control. Furthermore, SI algorithms are better than EA at recording and using historical data. Particle Swarm Optimization (PSO), Bat Inspired Algorithm (BA), Grey Wolf Optimization (GWO), Fruit Fly Optimization Algorithm (FOA), Moth-Flame Optimization (MFO), Ant Colony Optimization (ACO), Harris Hawks Optimizer (HHO), and ABC are examples of SI algorithms. In 2020, Li proposed SMA, a new stochastic optimization

The associate editor coordinating the review of this manuscript and approving it for publication was Mauro Gaggero.

algorithm based on the oscillation pattern of mucilage in literature [1]. The SMA mathematical model uses adaptive weights to simulate the process of generating positive and negative feedback from mucilage propagation waves based on biological oscillators, which results in the formation of the optimal path to connect food. SMA's exploration capability and development prospects have been validated through comparison. However, there are issues with slow convergence and easily falling into local optimal solutions.

With the increasing global energy shortage and environmental pollution, distributed power generation with clean fuel as energy is increasingly widely used in the power industry. Due to the increasing penetration rate of distributed power supply in power system, the power supply mode has a transition trend from large-scale centralized power supply to centralized and distributed power supply. Therefore, the research on DC distribution network under the new situation is one of the key problems to be solved urgently.

In DC distribution networks, MAs are widely used. In the literature [3], GA parameter identification is used to achieve accurate location of line faults in DC distribution networks, and the method is highly resistant to transition resistance and has high robustness. The algorithm, however, is prone to falling into local minima. The literature [4] proposed an improved genetic particle swarm algorithm by combining the PSO with the GA. The method combines the benefits of both the GA and the particle swarm method in global search, effectively integrating the two algorithms. The method is more resistant to interference and has higher localization accuracy and faster convergence speed. The simulated annealing algorithm, which has better global convergence and fault tolerance, was introduced in the literature [5]. However, the solution process of this algorithm is complicated and the optimization time is long.

In recent years, many improved optimization algorithms have outstanding performance [6], [7], [8]. Literature [9] combined SMA with the Adaptive Differential Evolution Algorithm (AGDE), and used the AGDE mutation method to improve the local search ability of population subjects, increase population diversity, and help avoid premature convergence; Chen et al [10] proposed an SVR-based prediction method using the K-mean clustering method and the Chaotic Slime Mould Algorithm (CSMA). The results show that the proposed method performs very well in terms of computational accuracy and complexity, but not in terms of stability; Ewees et al. proposed a new feature selection method in the literature [11] using a modified SMA based on the Firefly Algorithm (FA). FA improves convergence by improving the quality of the output results and is extremely capable of discovering the feasible domain of the optimal solution. The literature [12] proposed a binary version of the Binary Slime Mould Algorithm (BSMA) for feature selection to perform better feature selection and thus improve convergence speed. Experiments show that combining BSMA with Two-phase Mutation (TM) and a novel attack feeding strategy produces better results for feature selection. To address the potential shortcomings of SMA in handling nonlinear tasks, Rizk-Allah et al. [13] proposed a chaotic localization-enhanced slime mould algorithm (CO-SMA) based on Chaotic Search Strategy (CSS) and Cross Positioning Strategy (COS). CSS is introduced to improve the exploitation capability and thus avoid the problem of premature convergence; COS is introduced to improve the diversity of solutions and thus improve the exploratory tendency; Naik et al [14] proposed an elite-leadership-based SMA, which uses the global optimal solution to lead other individuals to update their positions, essentially solving the problem of inefficient exploitation and slow SMA convergence. Literature [15] proposed EOSMA, an equilibrium optimizer (EO)-guided SMA, to improve efficiency by optimizing the search of SMAs. In the literature [16], an improved SMA based on dominant swarm with adaptive t-distribution mutation (DTSMA) was proposed. In DTSMA, the dominant swarm is used to improve the SMA's convergence speed, and the adaptive t-distribution mutation balances is used to enhance the exploration and exploitation ability. In addition, a new exploitation mechanism is hybridized to increase the diversity of populations.

In conclusion, while the above improvement schemes employ various improvement algorithms to address the issues of slow convergence and poor search exploitation of SMA, there are still issues such as low convergence accuracy, easy premature convergence, and falling into local minima. Further improvements to the SMA are made in the literature [17], which combines the ABC with an improved crossover operator to form an adaptive ISMA. SMA's problems of slow convergence and easy falling into local minima were improved, but the above methods were not used to locate distribution network faults.

Aiming at the above research problems, this paper establishes a six-terminal ring distribution network model in Part II. In Part III, the short-circuit model is established and its mathematical expression is simplified. In Part IV and Part V of this paper, an adaptive ISMA with improved crossover operator is introduced for the fault location of DC distribution network. Based on the original SMA, ABC is introduced to solve the early convergence problem of the algorithm. ABC uses few control parameters and has strong robustness. Every iteration will search for global and local optimal solutions, so the probability of finding the optimal solution is greatly increased. Adaptive adjustable feedback factor and crossover operator are used to improve the convergence speed and accuracy of the algorithm. In addition, the advantages of ISMA are illustrated by the comparison of CEC2014 test functions. Part VI introduces the principle of fault location by ISMA. In Part VII of the paper, the experimental simulation is carried out, and the simulation results show that the improved algorithm has high positioning accuracy and robustness.

II. DC DISTRIBUTION NETWORK MODEL

Common DC distribution networks are classified into three types based on their basic topology: radial, two-end supply,

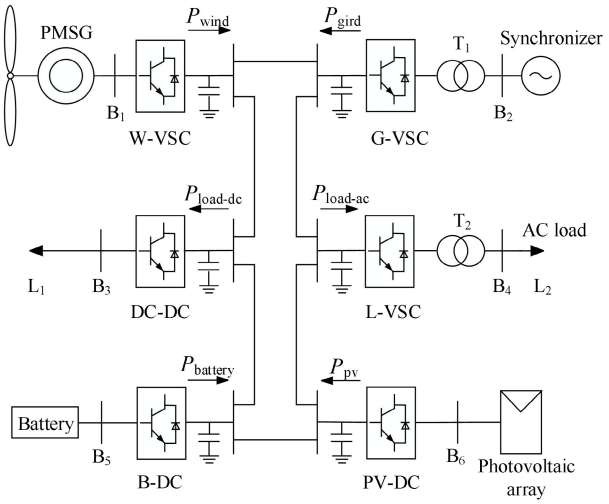

FIGURE 1. Topology of a six-terminal DC distribution network.

and ring. The relay protection and operation of a ring-shaped distribution network is more complicated, but the ring structure improves power supply reliability and does not affect the power supply to the load when a fault occurs in any section of the line within the ring to remove the faulty section. As a result, a six-terminal ring distribution network is used for the study in this paper, and its topological results are shown in Figure 1.

The wind turbine side, the synchronizer side, the battery side, the PV array side, and the DC and AC load sides are connected to a common DC bus through converters. Among them, the new energy generation unit is in the state of maximum power tracking to improve economic benefits; The DC load is connected to the DC bus through the buck-boost chopper converter; AC load is connected to DC bus through voltage source converter; The PV array unit is connected to the DC bus through a buck-boost chopper converter with bidirectional energy flow.

III. THE MATHEMATICAL MODEL FOR GRID LINE FAULTS

A. MATHEMATICAL MODEL OF INTER-POLE SHORT CIRCUIT FAULT

When an inter-pole short circuit fault occurs, the DC measuring capacitor discharges and the Insulate-Gate Bipolar Transistor (IGBT) is blocked due to its own protection device to prevent it from being burned and destroyed. However, the continuity diode still forms a circuit, and the DC and AC sides still supply current to the short circuit point [11].

Assuming an inter-pole short circuit fault in the DC line between G-VSC and W-VSC, the equivalent circuit of the capacitor discharge phase is shown in Figure 2.

In the figure, L indicates the total length of the DC line between the WTG end and the synchronous machine end; d indicates the distance between the WTG end and the fault point; R_1 and L_1 are the resistance and inductance between the WTG end and the fault point, respectively; R_2 and L_2 are the resistance and inductance between the synchronous machine

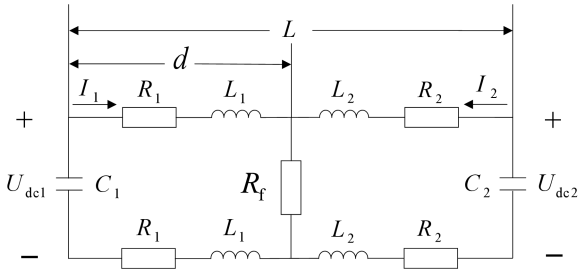

FIGURE 2. Equivalent circuit diagram of an inter-pole short circuit fault.

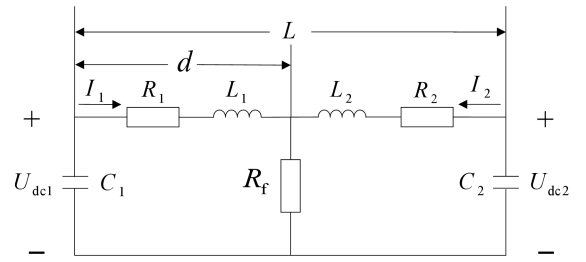

FIGURE 3. Equivalent circuit diagram of a unipolar short circuit fault.

end and the fault point, respectively; C_1 and C_2 are the capacitance to ground at the WTG end and the synchronous machine end, respectively; R_f is the transition resistance.

According to Kirchhoff's voltage theorem, the wind turbine terminal satisfies:

$$\begin{cases} U_{dc1} = 2I_1R_1 + 2L_1\dfrac{dI_1}{dt} + (I_1 + I_2)R_f \\ I_1 = C_1\dfrac{dU_{dc1}}{dt} \end{cases} \tag{1}$$

The synchronous machine side meets:

$$\begin{cases} U_{dc2} = 2I_2R_2 + 2L_2\dfrac{dI_2}{dt} + (I_1 + I_2)R_f \\ I_2 = C_2\dfrac{dU_{dc2}}{dt} \end{cases} \tag{2}$$

Combining Eq. (1) and Eq. (2) to eliminate the transition resistance R_f yields

$$2L_2C_2\frac{d^2U_{dc2}}{dt^2} - 2L_1C_1\frac{d^2U_{dc1}}{dt^2} + 2C_2R_2\frac{dU_{dc2}}{dt} - 2C_1R_1\frac{dU_{dc1}}{dt} + U_{dc1} - U_{dc2} = 0 \tag{3}$$

B. MATHEMATICAL MODEL OF SINGLE-POLE GROUNDED SHORT CIRCUIT FAULT

Assuming a single-pole ground short circuit fault in the DC line between G-VSC and W-VSC, the equivalent circuit for the capacitor discharge phase is shown in Figure 3.

According to Kirchhoff's voltage theorem, the wind turbine terminal satisfies:

$$\begin{cases} U_{dc1} = I_1R_1 + L_1\dfrac{dI_1}{dt} + (I_1 + I_2)R_f \\ I_1 = C_1\dfrac{dU_{dc1}}{dt} \end{cases} \tag{4}$$

The synchronous machine side meets:

$$\begin{cases} U_{dc2} = I_2 R_2 + L_2 \dfrac{dI_2}{dt} + (I_1 + I_2) R_f \\ I_2 = C_2 \dfrac{dU_{dc2}}{dt} \end{cases} \tag{5}$$

Combining Eq. (4) and Eq. (5) to eliminate the transition resistance R_f yields

$$L_2 C_2 \frac{d^2 U_{dc2}}{dt^2} - L_1 C_1 \frac{d^2 U_{dc1}}{dt^2} + C_2 R_2 \frac{dU_{dc2}}{dt} - C_1 R_1 \frac{dU_{dc1}}{dt} + U_{dc1} - U_{dc2} = 0 \tag{6}$$

C. DIFFERENTIAL VARIABLE TRANSFORMATION

In this paper, the differential quotient approximation of the finite difference method-derivative is used to express the differential components in terms of sampling points and sampling intervals. The sampling interval in this paper is 10 microseconds. Therefore, the 1st-order differential and 2nd-order differential in Eq. (7) can be transformed into, respectively.

$$\begin{cases} \dfrac{dU_{dc1}}{dt} = \dfrac{U_{dc}(k) - U_{dc}(k-2)}{2\Delta t} \\ \dfrac{d^2 U_{dc1}}{dt^2} = \dfrac{U_{dc}(k) - 2U_{dc}(k-1) + U_{dc}(k-2)}{\Delta t^2} \end{cases} \tag{7}$$

where k denotes the sampling point; $U_{dc}(k)$, $U_{dc}(k\text{-}1)$ and $U_{dc}(k\text{-}2)$ denote voltage sampling points at consecutive moments; and Δt denotes the sampling time interval.

IV. SLIME MOULD OPTIMIZATION ALGORITHM

SMA is based on the predatory behavior of slime mould, slime mould from the food source in response to the concentration of chemical signals encountered oscillating contraction, the higher the concentration of food encountered the faster its growth rate and the thicker the formation of the venous network, and conversely slime bacteria encountering a lower concentration of food will turn to explore other areas, so as to approach other food sources by the shortest route [17]. There are three main behaviors in the process of mucilage feeding: approaching food, wrapping food and acquiring food.

1) PROXIMITY TO FOOD

$$X(t+1) = \begin{cases} X_b(t) + v_b \times (W \times X_A(t) - X_B(t)), r < p \\ v_c \times X(t), r \geq p \end{cases} \tag{8}$$

where t is the current number of iterations, $X_B(t)$ is the position of the individual with the best current fitness, v_b and v_c are the control parameters, $v_b \in [-a, a]$, v_c oscillate between $[-1, 1]$ and eventually converge to 0, $X_A(t)$ and $X_B(t)$ are the positions of two random individuals, W is the slime adaptation weight, r is the random number between [0, 1], the expressions of the control parameters p, parameter a and the weight coefficient W are shown in Eq. (9), Eq. (10) and Eq. (11), and the variation curve of parameter a is shown in Figure 4 [15].

$$p = \tanh |S(i) - DF| \tag{9}$$

$$a = \operatorname{arctanh}(-(\frac{t}{t_{max}}) + 1) \tag{10}$$

$$W(SI(i)) = \begin{cases} 1 + r \cdot \log(\dfrac{bF - S(i)}{bF - wf} + 1) half \\ 1 - r \cdot \log(\dfrac{bF - S(i)}{bF - wf} + 1) others \end{cases} \tag{11}$$

$$SI(i) = sort(S) \tag{12}$$

where r is a random number between [0, 1], bF is the best fitness value of the current iteration, $S(i)$ is the fitness value of the current individual, wf is the worst fitness value of the current iteration, *half* is the individual in the top half of the population in terms of fitness, *others* is the remaining individuals in the population, and $SI(i)$ is the sequence of fitness values.

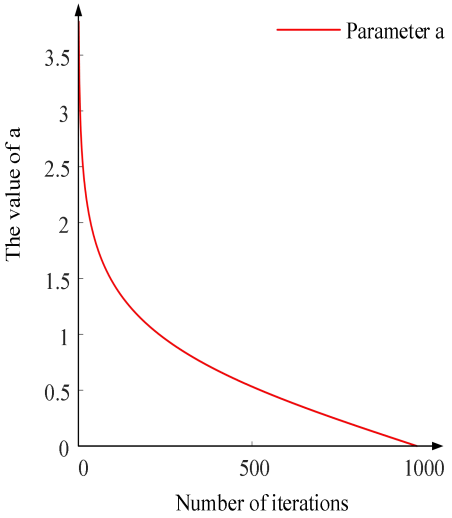

FIGURE 4. Schematic diagram of change curve of parameter a.

2) WRAPPING FOOD

After finding a high-concentration food source, the slime mould will separate some individuals to continue searching for a higher-concentration food source, so the slime bacteria population location update as shown in Eq. (13).

$$X(t+1) = \begin{cases} rand \cdot (UB - LB) + LB, rand < z \\ X_b(t) + v_b \cdot (W \cdot X_A(t) - X_B(t)), r < p \\ v_c \cdot X(t), r \geq p \end{cases} \tag{13}$$

where *rand* is a random number between [0, 1], *UB* and *LB* are the upper and lower bounds of the search area, and z is a custom parameter (typically 0.03).

3) ACCESS TO FOOD

The control parameter v_b oscillates randomly between [−a, a] and eventually converges to 0 as the number of iterations increases. the control parameter v_c oscillates randomly

between [−1, 1] and eventually converges to 0 as the number of iterations increases.

The process of SMA is shown in Figure 5

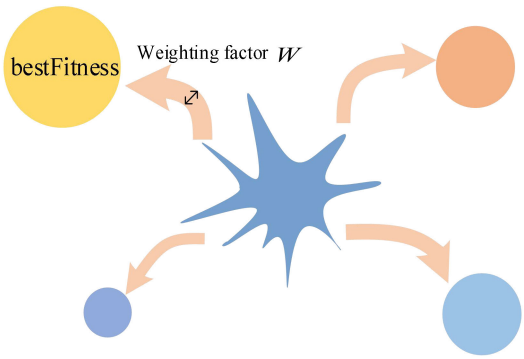

FIGURE 5. Schematic diagram of slime mould predation process.

V. MULTI-STRATEGY IMPROVEMENT OF SLIME MOULD OPTIMIZATION ALGORITHM

A. ADAPTIVE FEEDBACK FACTOR

v_c as the feedback factor should reflect the relationship between slime mass and food concentration, oscillating between [−1, 1] and eventually converging to 0. The size of v_c at this time is only related to the number of iterations and does not accurately represent the relationship between slime mass and food concentration, so the adaptive adjustable feedback factor is introduced [18]. In the early iteration of the algorithm, the food concentration is low, and the decreasing speed of the feedback factor should be accelerated to weaken the feedback relationship and improve the search efficiency. In the late iteration of the algorithm, the food concentration is high, and the feedback factor should be kept smooth at this time, which is beneficial to the local search. In addition, the descent rate adjustment factor k is introduced to automatically adjust the descent rate of the feedback factor. The mathematical model of the adaptive adjustable feedback factor is described as shown in Eq. (14).

$$v_c = \left(\frac{e^{\frac{t_{\max} - t}{t_{\max}}} - 1}{e - 1} \right)^k \tag{14}$$

The word where t is the current number of iterations, $t_{\max}$ is the maximum number of iterations, and k is the adjustment factor.

A graph of the variation of the feedback factor v_c with the number of iterations for different values of k is shown in Figure 6.

As can be seen from Fig. 6, the rate of decrease of the feedback factor v_c increases with the increase of the regulation factor k. However, if the regulation factor is too large, the convergence rate of the first period is too fast. However, if the adjustment factor k is too large, the convergence speed is too fast in the early stage and it is easy to fall into the local minimum. On the contrary, if the adjustment factor k is too small, it will cause the problem that the convergence speed

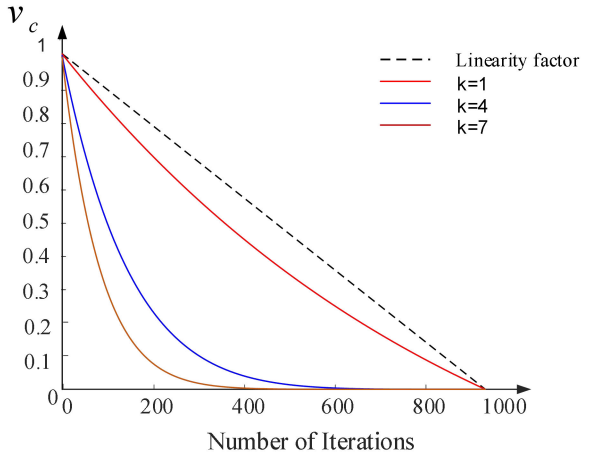

FIGURE 6. Feedback factor curve.

is too slow and the advantage of the algorithm disappears. Considering all aspects, 0.4 is chosen as the value of the adjustment factor k.

B. IMPROVED ARITHMETIC CROSS OPERATOR

To speed up the convergence of the algorithm, an improved arithmetic crossover operator is introduced to let the current individual cross over with a certain probability with the most available individuals in the population, and its mathematical model is shown in Eq. (15).

$$\begin{cases} X_{A1}(t+1) = L \cdot X_A(t) + (1-L) \cdot X_{best}(t) \\ X_{A2}(t+1) = L \cdot X_{best}(t) + (1-L) \cdot X_A(t) \end{cases} \tag{15}$$

where t is the current number of iterations, X_A is the current individual position, X_{A1} and X_{A2} are the positions of the individuals of the two children generated by the crossover, X_{best} is the position of the optimal individual of the current population, and L is a random parameter taking the value (0,1).

From Eq. (15), it can be learned that the offspring are mainly determined by the parent and parameter L. In order to enhance the population diversity, the Laplace coefficient is introduced to improve the control parameter L. The mathematical model is shown in Eq. (16).

$$L = \begin{cases} \mu - \lambda \cdot \ln(r), r \le \frac{1}{2} \\ \mu + \lambda \cdot \ln(r), r > \frac{1}{2} \end{cases} \tag{16}$$

where μ and λ are Laplace coefficients and μ is taken as a natural number to control the position. $\lambda > 0$ is used to control the scale and r is taken as a random number between [0, 1]. From Eq.16, it is clear that the smaller λ is, the closer the offspring is to the parent. With the joint mediation of Laplace coefficients μ and λ, the offspring can selectively acquire more information of the superior parent.

C. IMPROVED MANUAL SWARM SEARCH STRATEGY

ABC algorithm is a popular local optimization-seeking intelligence algorithm that solves the optimization problem by

mimicking the behavior of honey bee populations that can efficiently harvest honey and adapt to environmental changes in any environment [19]. The algorithm classifies artificial bee colonies into three categories: honey collecting bees, observation bees and detection bees. Honey collecting bees correspond to nectar sources one by one and use nectar information to share with observation bees; observation bees wait in the hive and search for new nectar sources based on nectar information from collecting bees; and scout bees randomly search for new nectar sources near the hive. The algorithm does not require special information about the problem and has generality as well as faster convergence, which can effectively solve the problem of early convergence of the SMA [20], [21]. The basic artificial bee colony search strategy mathematical model is described as shown in Eq. (17).

$$z_{id} = x_{id} + \phi_{id}(x_{id} - x_{kd}) \tag{17}$$

where i is the current number of nectar sources, z_{id} is the new optimal individual, x_{id} is the current individual, x_{kd} is a random individual, $k \in \{0, 1, \ldots, M\}$, $d \in \{1, 2, \ldots, N\}$, M is a fixed value, and N is the dimension.

In order to better improve the development capability of the algorithm, the optimal position guidance is introduced in this paper, and the improved mathematical model is shown in Eq. (18).

$$z_{id} = x_{id} + \phi_{id}(x_{id} - x_{kd}) + r_{id}(p_{gd} - x_{id}) \tag{18}$$

where r is a random number between [0, 1.5] and p_g is the global optimal position.

D. ISMA WORKFLOW

(1) Initialize the location of the mucilage population and set parameters such as upper and lower boundaries.

(2) Calculate the fitness of individuals in the population and record the best fitness and the worst fitness.

(3) Calculate the values of each parameter and the weights of individuals within the population.

(4) Determine whether the probability requirement is satisfied, and if so, perform the crossover operation, if not, update the best fit and best position.

(5) Introducing an improved artificial bee colony search strategy to retain the best individuals according to a greedy strategy.

(6) Determine whether the maximum number of iterations is reached, and if it is satisfied, output the best adaptation and the best position; if not, repeat steps (3) to (5)

The ISMA flow chart is shown in Figure 7.

E. THE COMPLEXITY OF ISMA

The complexity of the algorithm is obtained by analyzing the code line by line. The complexity behind each line of code is marked. Finally, the complexity of ISMA is O(n^3). Similarly, the complexity of SMA is O(n^3). Under the same complexity, ISMA convergence requires fewer iterations and takes less time.

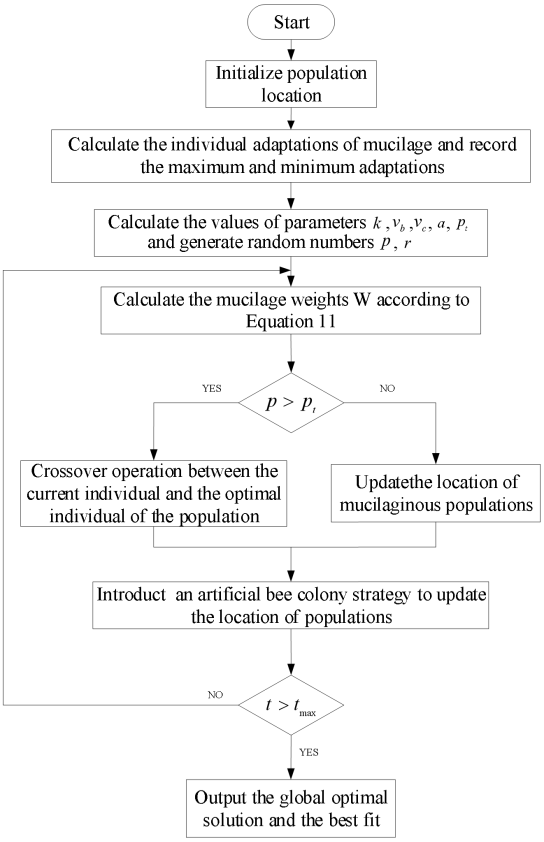

FIGURE 7. ISMA flow chart.

TABLE 1. Part of the CEC2014 function.

Function	Dim	Characteristic	Range	f_{min}
CEC03	30	UN	[-100,100]	500
CEC06	30	MF	[-100,100]	600
CEC19	30	HF	[-100,100]	1900
CEC26	30	CF	[-100,100]	2600

F. COMPARISON OF CEC2014 TEST FUNCTION OPTIMIZATION

In order to verify the performance of ISMA in solving optimization problems, we selected CEC03, CEC06, CEC19 and CEC26 in the CEC2014 test set as the test functions. It includes Unimodal Functions(UF), Simple Multimodal Functions(MF), and Hybrid Functions(HF) and Composition Functions(CF). Relevant information of CEC2014 test function is shown in the following table 1. The experimental parameters are as follows: population size N = 50, dimension d = 30, maximum number of iterations t_{max} = 2000, and each function runs independently for 30 times to get the average and standard deviation. In this paper, PSO algorithm, GWO algorithm, SMA and ISMA are selected to compare the optimization results, among which the experimental data of PSO algorithm and GWO algorithm are from the literature [1] and literature [17] respectively. The comparative analysis of the optimization results of CEC2014 test function by each algorithm is shown in the following table 2.

According to the results in the table, 1 SMA shows some advantages in solving function optimization. For CEC19

function, ISMA can find the optimal value, and for other mixed and composite CEC2014 functions, ISMA can also converge to the optimal value, which shows that ISMA is also very robust in dealing with complex problems.

VI. FAULT LOCATION IN DC DISTRIBUTION NETWORK BASED ON ADAPTIVE ARTIFICIA BEE COLONY SLIME MOULD ALGORITHM

First, the inductance and resistance per unit length are used to express the line parameters, as shown in Eq. (19).

$$\begin{cases} R_1 = r \cdot d \\ L_1 = l \cdot d \\ R_2 = r \cdot (L - d) \\ L_2 = l \cdot (L - d) \end{cases} \tag{19}$$

where r denotes the resistance per unit length of line; l denotes the inductance per unit length of line.

Substituting Eq. (7) and Eq. (19) into Eq. (3) and Eq. (6), we get:

$$2LC(lb_2 + ra_2) - 2dC(lb + ra) + \Delta U = 0 \tag{20}$$

$$LC(lb_2 + ra_2) - dC(lb + ra) + \Delta U = 0$$

$$\begin{cases} a_1 = \dfrac{\mathrm{d}U_{\mathrm{dc1}}}{\mathrm{d}t} = \dfrac{U_{\mathrm{dc1}}(k) - U_{\mathrm{dc1}}(k-2)}{2\Delta t} \\ a_2 = \dfrac{\mathrm{d}U_{\mathrm{dc2}}}{\mathrm{d}t} = \dfrac{U_{\mathrm{dc2}}(k) - U_{\mathrm{dc2}}(k-2)}{2\Delta t} \\ b_1 = \dfrac{\mathrm{d}^2U_{\mathrm{dc1}}}{\mathrm{d}t^2} = \dfrac{U_{\mathrm{dc1}}(k) - 2U_{\mathrm{dc1}}(k-1) + U_{\mathrm{dc1}}(k-2)}{\Delta t^2} \\ b_2 = \dfrac{\mathrm{d}^2U_{\mathrm{dc2}}}{\mathrm{d}t^2} = \dfrac{U_{\mathrm{dc2}}(k) - 2U_{\mathrm{dc2}}(k-1) + U_{\mathrm{dc2}}(k-2)}{\Delta t^2} \\ \Delta U = U_{\mathrm{dc1}} - U_{\mathrm{dc2}} \end{cases} \tag{21}$$

The fitness function $S(d)$ is set as:

$$S(d) = \sum_{k=1}^{N-1} f_k^2(d) \tag{22}$$

Depending on the different fault cases that occur, $f_k(d)$ is the left-hand part of (20) or (21). $f_k(d)$ has a theoretical value of 0. The larger the fitness function, the stronger the fitness. The specific process is shown in Figure 8.

VII. SIMULATION VERIFICATION

In this paper, a six-terminal ring distribution network is built in MATLAB/SIMULINK platform for simulation and validation, using double closed-loop PI control. The rated voltage of the system is 500kV, and both positive and negative shunt capacitors are 0.02F. The distribution network lines are simulated using a centralized R-L parameter model.

A. PARAMETER SETTING

The specific parameters of the model are shown in Table 3.

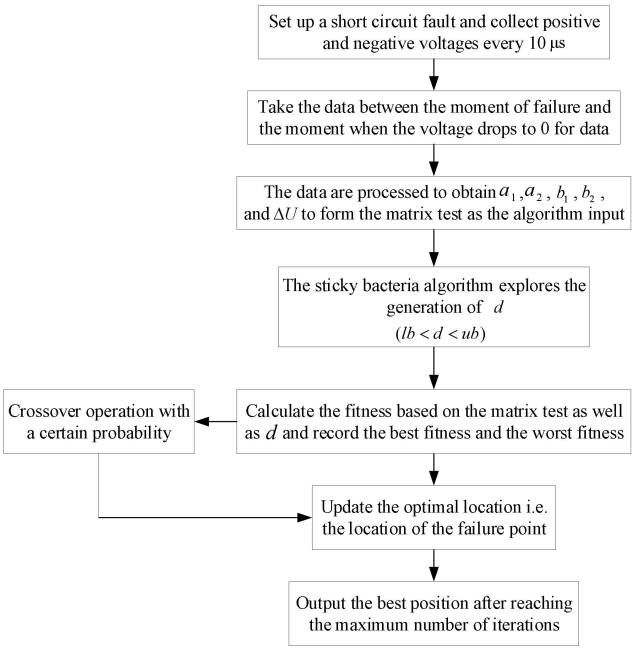

FIGURE 8. Flow chart of fault location based on adaptive artificial bee colony slime mould algorithm.

B. FAULT LOCATION RESULTS AND ANALYSIS

On the basis of the six-end ring distribution network, the DC line between the wind turbine end and the synchronous machine end was selected as the research object. The results are shown in Table 4 and Table 5, where the ranging error is calculated as shown in Eq. (23).

$$r = \frac{|x_c - x_r|}{L} \times 100\% \tag{23}$$

where r represents the ranging error, x_c represents the calculated ranging result, x_r represents the actual fault distance, and L represents the total line length.

From the experimental results, it can be seen that the fault location by applying the ISMA can control the error below 2% when there is no transition resistance, and below 3% when the transition resistance is 10Ω.

Taking the failure point at 5 km as an example, 1000 points in Fig. 9 are used to simulate 1000 individual slime mould in the population. As the algorithm advances and keeps searching for the best, most of the 1000 mould are distributed on this line, i.e., the location is accurate. The results are shown in Figure 10.

C. ALGORITHM COMPARISON ANALYSIS

In this paper, the PSO algorithm, GWO algorithm, SMA and ISMA are selected for experimental comparison, and the parameters are uniformly set to the maximum number of iterations 500 and the number of individuals in the population 1000. the simulation experiments are conducted at the fault point of 5 km, and the results are shown in Figure 11.

From the simulation results of Figure 11, it can be seen that the convergence speed of ISMA is obviously faster than other algorithms, and it converges within 10 iterations. The

TABLE 2. CEC2014 function optimization comparison.

Function	PSO		GWO		SMA		ISMA	
	AVG	STD	AVG	STD	AVG	STD	AVG	STD
CEC03	4.87E+01	6.61E+01	5.21E+02	5.11E-02	5.21E+02	2.27E-01	4.88E+02	3.34E+03
CEC06	1.08E+01	2.53E+00	6.14E+02	3.27E+00	6.15E+02	3.06E+00	6.17E+02	3.55E+00
CEC19	7.96E+01	1.87E+00	1.96E+03	3.93E+01	1.92E+03	2.09E+01	1.90E+03	2.17E+01
CEC26	1.07E+02	2.49E+01	2.77E+03	6.85E+01	2.70E+03	1.11E-01	2.70E+03	1.60E-01

TABLE 3. Partial parameters of DC distribution network system.

Model Parameters	Numerical value
DC bus voltage /V	500
Line length /km	10
DC side shunt capacitance value / F	0.02
Inductance per unit length of line / $H \cdot km^{-1}$	1.59×10^{-4}
Unit length line resistance value / $\Omega \cdot km^{-1}$	1.39×10^{-2}
Sampling interval / μs	10

TABLE 4. Partial parameters of DC distribution network system.

Fault Type	Transition Resistors /Ω	Actual value /km	Positioning value /km	Error
Bipolar short circuit fault	0	1	0.9524	0.476%
		3	2.8841	1.159%
		5	5.1158	1.158%
		7	7.0043	0.043%
		9	8.9415	0.585%
	10	1	0.9219	0.781%
		3	3.1971	1.971%
		5	4.8267	1.733%
		7	7.0000	0%
		9	8.7369	2.631%

TABLE 5. Location results of single-pole short-circuit fault.

Fault Type	Transition Resistors /Ω	Actual value /km	Positioning value /km	Error
Single pole ground short circuit fault	0	1	0.9855	0.145%
		3	2.9549	0.451%
		5	5.1206	1.206%
		7	7.1132	1.132%
		9	8.9536	0.464%
	10	1	0.8944	1.056%
		3	3.0247	0.247%
		5	5.1020	1.020%
		7	7.2635	2.635%
		9	8.8636	1.364%

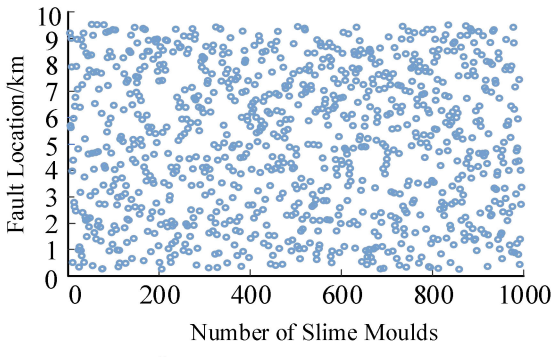

FIGURE 9. The initial state distribution of slime mould population.

PSO algorithm and GWO algorithm are expected to converge after hundreds of iterations. This further proves that the

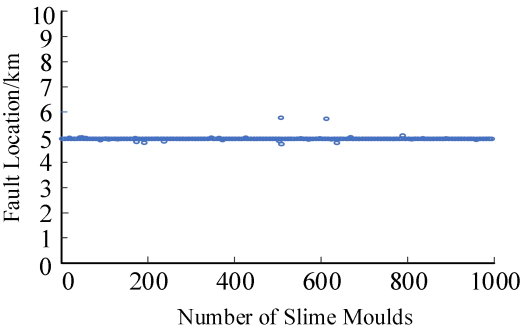

FIGURE 10. The final state distribution of slime mould population.

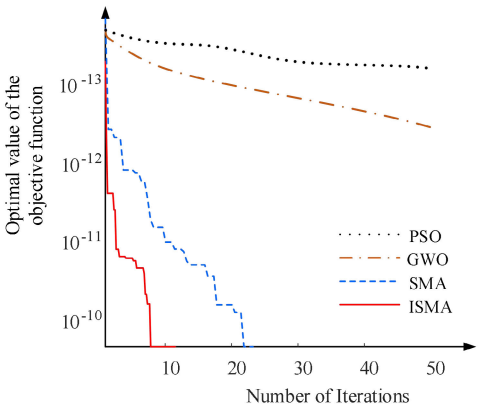

FIGURE 11. Comparison of convergence of different algorithms.

effectiveness of ISMA has great advantages over basic PSO algorithm, GWO algorithm, SMA and ISMA in solving this problem.

VIII. CONCLUSION

In this paper, we first establish a mathematical model for bipolar short-circuit faults as well as single-pole grounded short-circuit faults in DC distribution networks, eliminate the influence of transition resistance theoretically through the fault characteristic formula, and discretize the differential components in the formula. The test matrix is defined as the parameters of ISMA. Then the six-terminal ring distribution network is built in MATLAB/SIMULINK platform for experimental simulation, and the voltage and current values of the obtained sampling points are composed of the test matrix by operation to further obtain the adaptation function and finally calculate the fault location. The experimental results are compared with the actual data, and the experimental results show that ISMA can control the error of fault location within 2% without transition resistance and below 3% when the transition resistance is 10Ω. PSO algorithm, GWO algorithm,

SMA and ISMA are selected for experimental comparison with the fault point at 5 km. The results show that ISMA can obtain the optimal solution in a shorter time compared with other algorithms, which further indicates that ISMA has strong practicality and robustness in solving DC distribution network faults.

Prospect I: Many excellent algorithms have been proposed but have not been used in fault location of distribution network. How to use these algorithms to locate the distribution network more accurately needs further study.

Prospect II: This paper is based on the ring distribution network. However, the distribution network structure is diverse, such as petal distribution network adopted in recent years. The work of fault location for distribution networks with different structures needs further study.

REFERENCES

[1] S. Li, H. Chen, M. Wang, A. A. Heidari, and S. Mirjalili, "Slime mould algorithm: A new method for stochastic optimization," *Future Gener. Comput. Syst.*, vol. 111, pp. 300–323, Oct. 2020.
[2] G. Beni and J. Wang, "Swarm intelligence in cellular robotic systems," in *Proc. Meeting Robot. Soc. Jpn.*, 1993.
[3] S. Jamali, A. Bahmanyar, and H. Borhani-Bahabadi, "A fast and accurate fault location method for distribution networks with dg using genetic algorithms," in *Proc. Smart Grid Conf. (SGC)*, Dec. 2015, pp. 110–114.
[4] A. Mahmoudian and M. Niasati, "A novel approach for optimal allocation of fault current limiter in distribution system via combination of particle swarm optimization algorithm and genetic algorithm (PSOGA)," in *Proc. 21st Conf. Electr. Power Distrib. Netw. Conf. (EPDC)*, Apr. 2016, pp. 75–81.
[5] X. Mi, S Ying, and K. Li, "Fault location of distribution networks based on fuzzy adaptive simulated annealing genetic algorithm," *Elect. Meas. Instrum.*, vol. 53, pp. 44–48, Sep. 2016.
[6] L. Ma, S. Cheng, and Y. Shi, "Enhancing learning efficiency of brain storm optimization via orthogonal learning design," *IEEE Trans. Syst. Man, Cybern. Syst.*, vol. 51, no. 11, pp. 6723–6742, Nov. 2021.
[7] H. Yu, T. Xu, X. Wang, X. Yi, and J. Chen, "Large-scale weapon target assignment based on improved MOEA/D algorithm," in *Proc. 4th Int. Conf. Syst. Rel. Saf. Eng. (SRSE)*, Dec. 2022, pp. 86–91.
[8] Z. H. Tong, Z. C. Sheng, Z. Bin, D. P. Bo, and Y. Yang, "Decomposition-based sub-problem optimal solution updating direction-guided evolutionary many-objective algorithm," *Inf. Sci.*, vols. 448–449, pp. 91–111, Jun. 2018.
[9] E. H. Houssein, M. A. Mahdy, M. J. Blondin, D. Shebl, and W. M. Mohamed, "Hybrid slime mould algorithm with adaptive guided differential evolution algorithm for combinatorial and global optimization problems," *Expert Syst. Appl.*, vol. 174, Jul. 2021, Art. no. 114689.
[10] Z. Chen and W. Liu, "An efficient parameter adaptive support vector regression using K-means clustering and chaotic slime mould algorithm," *IEEE Access*, vol. 8, pp. 156851–156862, 2020.
[11] A. A. Ewees, L. Abualigah, D. Yousri, Z. Y. Algamal, M. A. A. Al-Qaness, R. A. Ibrahim, and M. A. Elaziz, "Improved slime mould algorithm based on firefly algorithm for feature selection: A case study on QSAR model," *Eng. With Comput.*, vol. 38, no. S3, pp. 2407–2421, Aug. 2022.
[12] M. Abdel-Basset, R. Mohamed, R. K. Chakrabortty, M. J. Ryan, and S. Mirjalili, "An efficient binary slime mould algorithm integrated with a novel attacking-feeding strategy for feature selection," *Comput. Ind. Eng.*, vol. 153, Mar. 2021, Art. no. 107078.
[13] R. M. Rizk-Allah, A. E. Hassanien, and D. Song, "Chaos-opposition-enhanced slime mould algorithm for minimizing the cost of energy for the wind turbines on high-altitude sites," *ISA Trans.*, vol. 121, pp. 191–205, Feb. 2022.
[14] M. K. Naik, R. Panda, and A. Abraham, "Normalized square difference based multilevel thresholding technique for multispectral images using leader slime mould algorithm," *J. King Saud Univ. Comput. Inf. Sci.*, vol. 34, no. 7, pp. 4524–4536, Jul. 2022.
[15] S. Yin, Q. Luo, and Y. Zhou, "EOSMA: An equilibrium optimizer slime mould algorithm for engineering design problems," *Arabian J. Sci. Eng.*, vol. 47, no. 8, pp. 10115–10146, Aug. 2022.
[16] S. H. Yin, Q. F. Luo, and Y. Q. Zhou, "Dominant swarm with adaptive T-distribution mutation-based slime mould algorithm," *Math. Biosci. Eng.*, vol. 19, no. 3, pp. 2240–2285, 2022.
[17] C. H. Liu and Q. He, "Improved crossover operator for adaptive artificial bee colony sticky fungus algorithm," *Small Microcomput. Syst.*, vol. 44, pp. 263–268, Feb. 2023.
[18] K. Deep and M. Thakur, "A new crossover operator for real coded genetic algorithms," *Appl. Math. Comput.*, vol. 188, no. 1, pp. 895–911, May 2007.
[19] X. Bing, Z. Youwei, Z. Xueyan, and S. Xuekai, "An improved artificial bee colony algorithm based on faster convergence," in *Proc. IEEE Int. Conf. Artif. Intell. Comput. Appl. (ICAICA)*, Jun. 2021, pp. 776–779.
[20] X. Sun, Z. Shen, J. Jing, and S. Zhao, "Fault location method of active distribution network based on improved artificial bee colony algorithm," in *Proc. IEEE 10th Joint Int. Inf. Technol. Artif. Intell. Conf. (ITAIC)*, vol. 10, Jun. 2022, pp. 163–167.
[21] Z. H. Mei, P. M. Fang, and Z. Liang, "Fault location based on artificial bee colony algorithm for distribution network with distributed generators," *Adv. Mater. Res.*, vol. 787, pp. 840–845, Jan. 2013.

TIAN-XIANG MA was born in 1986. He is currently pursuing the master's degree. He is also a senior engineer. He is mainly engaged in the research of operation and control of distribution system and the key technology of distribution network equipment.

XIN DUAN was born in 1989. He is currently pursuing the master's degree. He is mainly engaged in analysis and management of distribution network operation, and research on distribution automation technology.

YAN XU was born in 1976. He received the Ph.D. degree from the North China University of Electric Power, in 2005. He is currently an associate professor. His research interests include power system relay protection and new energy grid connection technology.

RUO-LIN WANG was born in 1999. She is currently pursuing the master's degree with the Department of Electric Power Engineering, North China Electric Power University. Her research interest includes DC distribution network fault location.

XIAO-YU LI was born in 1994. She is currently pursuing the master's degree. She is mainly engaged in the analysis and management of distribution network operation, and the research of distribution automation technology.